Equations of state of $GdFeO_3$ and $GdAlO_3$ perovskites

2004 J. Phys.: Condens. Matter 16 5721

(http://iopscience.iop.org/0953-8984/16/32/009)

INSTITUTE OF PHYSICS PUBLISHING JOURNAL OF PHYSICS: CONDENSED MATTER

J. Phys.: Condens. Matter **16** (2004) 5721–5730 PII: S0953-8984(04)79278-4

Equations of state of $GdFeO_3$ and $GdAlO_3$ perovskites

N L Ross[1,3], J Zhao[1], J B Burt[1] and T D Chaplin[2]

[1] Crystallography Laboratory, Department of Geosciences, Virginia Polytechnic Institute and State University, Blacksburg, VA 24061, USA
[2] Department of Chemistry, University College London, Gower Street, London WC1E 6BT, UK

E-mail: nross@vt.edu

Received 15 April 2004
Published 30 July 2004
Online at stacks.iop.org/JPhysCM/16/5721
doi:10.1088/0953-8984/16/32/009

Abstract

The structures of orthorhombic $GdAlO_3$ and $GdFeO_3$ perovskites have been refined at room temperature and pressure using single-crystal x-ray diffraction and their equations of state have been measured to pressures of 7.95 and 7.58 GPa, respectively. Both structures are distorted through the tilting and distortion of the octahedra. $GdAlO_3$ is less distorted than $GdFeO_3$ with an average Al–O–Al tilt angle of 156.42(16)° compared to an average Fe–O–Fe tilt angle of 147.10(10)° in $GdFeO_3$. Both the FeO_6 octahedra and GdO_{12} sites in $GdFeO_3$ are more distorted than those in $GdAlO_3$. Neither perovskite exhibits any phase transitions throughout the pressure range studied. A fit of a third-order Birch–Murnaghan equation of state to the P–V data yields values of $K_{T0} = 191(1)$ GPa and $K'_0 = 5.8(3)$ for $GdAlO_3$ and $K_{T0} = 182(1)$ GPa and $K'_0 = 6.3(3)$ for $GdFeO_3$. Analysis of the unit cell parameter data shows that [100] is least compressible in both compounds and that $GdFeO_3$ compresses more isotropically than $GdAlO_3$. The compressional moduli for the unit cell parameters of $GdFeO_3$ are $K_{a0} = 188(3)$ GPa, $K_{b0} = 181(1)$ GPa and $K_{c0} = 177(2)$ GPa, with $K'_{a0} = 5.2(7)$, $K'_{b0} = 5.7(4)$ and $K'_{c0} = 8.2(5)$, compared with $K_{a0} = 234(5)$ GPa, $K_{b0} = 151(2)$ GPa and $K_{c0} = 205(1)$ GPa, with $K'_{a0} = 12(1)$, $K'_{b0} = 3.8(4)$ and $K'_{c0} = 4.7(2)$ for $GdAlO_3$. There is no significant change in the pseudocubic unit cell parameters with pressure in $GdFeO_3$ whereas they converge in $GdAlO_3$. In particular, the a_c and b_c are predicted to merge by 12 GPa, signifying a possible transition from orthorhombic to tetragonal symmetry.

[3] Author to whom any correspondence should be addressed.

1. Introduction

Oxide perovskites with general stoichiometry ABO_3 are relatively simple structures comprised of corner-linked BO_6 cation-centred octahedra with larger A cations occupying the voids within the three-dimensional framework of octahedra. In the ideal cubic perovskite structure, the A cations are surrounded by twelve equidistant oxygen ions. Many ABO_3 compounds crystallize with the orthorhombic distortion of the perovskite structure and $GdFeO_3$ is considered to be the prototype of this series. The orthorhombic structures are derived from the ideal cubic structure via the titling and distortion of the BO_6 octahedra (e.g. [1–3]). Perovskites are of great interest in materials science because the relatively simple crystal structure displays many diverse electric, magnetic, piezoelectric, optical, catalytic and magnetoresistive properties. In addition, perovskites are of interest in Earth sciences because $(Mg, Fe)SiO_3$ transforms to a perovskite structure with $Pbnm$ symmetry at high pressures and temperatures and is believed to form the bulk of the Earth's lower mantle (e.g. [4]).

This paper presents a comparison of the $GdFeO_3$ and $GdAlO_3$ perovskites made in order to explore the effect that substitution for Al^{3+} with Fe^{3+} has on the distortion and compressibilities of the structures. The structure of $GdFeO_3$ perovskite has been previously refined by Geller [5] and improved by Marezio *et al* [6], but a high quality structure refinement for $GdAlO_3$ perovskite is lacking. In order to compare the two structures, we refined both structures under ambient conditions in air using single-crystal x-ray diffraction. We also report the equations of state of the two perovskites determined by high pressure single-crystal x-ray diffraction at room temperature. Such studies provide insight into the atomistic controls on the structural changes in this important class of materials.

2. Experimental procedures

2.1. Refinements under ambient conditions

$GdFeO_3$ and $GdAlO_3$ crystals were kindly provided by the Department of Mineral Sciences, Natural History Museum of the Smithsonian Institution. Each crystal was hand-picked, with crystal sizes of $150 \times 120 \times 35\ \mu m^3$ ($GdFeO_3$) and $172 \times 76 \times 30\ \mu m^3$ ($GdAlO_3$). Unit cell parameters for $GdFeO_3$ and $GdAlO_3$ were obtained from a Huber four-circle diffractometer using filtered Mo Kα radiation, measuring between 21 and 30 reflections centred at eight equivalent positions following the procedure of King and Finger [7]. X-ray intensity data sets for both crystals were obtained from the Xcalibur 1 single-crystal diffractometer, using monochromatized Mo Kα radiation ($\lambda = 0.709\,26$ Å) with a tube power of 50 kV and 40 mA, under atmospheric conditions. The data sets were collected with an omega scan of $0.05^\circ\ s^{-1}$, scan width of 1.2° and a step number of 60. The peaks were integrated by the program WinIntegrStp [8] which performs a full peak-profiling of the step-scan data by the methods of Pavese and Artioli [9]. Integrated intensities were corrected for absorption using a modified version of ABSORB [10]. The ranges of crystal transmission for the $GdFeO_3$ and the $GdAlO_3$ were 0.069–0.358 and 0.062–0.333, respectively. Symmetrically equivalent reflections were then averaged according to the Laue symmetry mmm. R(int) values for the 630 averaged reflections for $GdAlO_3$ and the 891 averaged reflections for $GdFeO_3$ are given in table 1.

Crystal structure refinements were carried out using RFINE99 developed by Angel from the previous RFINE4 code by Finger and Prince [11]. The program utilizes a full-matrix least squares refinement using scattering factors and coefficients for dispersion corrections from the International Tables for Crystallography. The details of the refinements are given in table 1, atomic positions and displacement parameters for $GdAlO_3$ and $GdFeO_3$ are given in tables 2 and 3, respectively, and selected bond lengths and angles are given in table 4.

Table 1. Details of least squares structure refinements at room pressure and temperature for $GdAlO_3$ and $GdFeO_3$ perovskites.

	Compound	
	$GdAlO_3$	$GdFeO_3$
Space group	*Pbnm*	*Pbnm*
Crystal size (μm)	150 × 120 × 35	172 × 76 × 30
a (Å)	5.253 68(11)	5.351 05(23)
b (Å)	5.303 04(10)	5.612 49(10)
c (Å)	7.443 46(24)	7.671 06(11)
V (Å^3)	207.414(9)	230.384(10)
Z	4	4
ρ_{calc} (g cm^{-3})	7.436	7.527
λ (Å)	0.709 26	0.709 26
μ (mm^{-1})	32.26	34.84
θ range for data collection	2°–40°	2°–45°
Limiting indices	$-9 \leqslant h \leqslant 9$, $-9 \leqslant k \leqslant 9$, $0 \leqslant l \leqslant 13$	$-10 \leqslant h \leqslant 10$, $0 \leqslant k \leqslant 10$, $-14 \leqslant l \leqslant 14$
No of refl. $>2I_0/\sigma(I_0)$	2247	3107
No of ind. refl. ($F > 4\sigma(F)$)	630	891
R_{int} [a]	0.0243 (605)	0.023 2 (857)
No of parameters	29	29
G_{fit} [b]	1.30	0.92
Extinction factor ($\times 10^{-4}$)	0.065(4)	0.075(4)
R_w [c]	0.032	0.026
R [d]	0.028	0.019

[a] Internal residual on F (number of averaged reflections).
[b] G_{fit}: estimated standard deviation of unit weight observation.
[c] $R_w = [\sum w(|F_0| - |F_c|)^2 / \sum |F_0|^2]^2$.
[d] $R = \sum ||F_0| - |F_c|| / \sum |F_0|$.

Table 2. Positional, equivalent isotropic displacement parameters (β_{iso}) and anisotropic displacement parameters (β_{ij}) for $GdAlO_3$ perovskite.

Atom	Site	x	y	z	β_{iso}	
Gd	4c	−0.007 93(3)	0.037 63(4)	0.25	0.3801	
Al	4b	0	0.5	0	0.2829	
O1	4c	0.072 4(6)	0.486 3(6)	0.25	0.4578	
O2	8d	0.714 7(4)	0.285 5(3)	0.0387(3)	0.4436	
Atom	β_{11}	β_{22}	β_{33}	β_{12}	β_{13}	β_{23}
Gd	0.003 25(8)	0.003 25(9)	0.001 88(4)	−0.000 36(3)	0.0	0.0
Al	0.002 5(4)	0.002 6(3)	0.001 3(2)	−0.000 2(2)	0.0000(2)	0.0004(3)
O1	0.003 7(7)	0.005 2(7)	0.001 7(4)	0.000 5(7)	0.0	0.0
O2	0.003 6(5)	0.002 7(4)	0.002 8(3)	−0.001 2(4)	0.0005(3)	−0.0004(3)

2.2. Equations of state

Single crystals of $GdAlO_3$ and $GdFeO_3$ perovskite suitable for high pressure studies were chosen on the basis of their optical and diffraction quality. The high pressure measurements were performed with a BGI-design diamond anvil cell [12] using T301 steel as a gasket. Crystals of $GdAlO_3$ and $GdFeO_3$ were loaded into the diamond anvil cell together with a ruby

Table 3. Positional, equivalent isotropic displacement parameters and anisotropic displacement parameters for $GdFeO_3$ perovskite.

Atom	Site	x	y	z	β_{iso}	
Gd	4c	−0.015 39(3)	0.062 59(2)	0.25	0.4186	
Fe	4b	0	0.5	0	0.3475	
O1	4c	0.100 9(5)	0.466 9(4)	0.25	0.4693	
O2	8d	0.696 6(3)	0.301 1(3)	0.0518(2)	0.4986	
Atom	β_{11}	β_{22}	β_{33}	β_{12}	β_{13}	β_{23}
Gd	0.003 83(5)	0.003 26(4)	0.001 72(2)	0.000 45(2)	0.0	0.0
Fe	0.003 01(9)	0.003 08(10)	0.001 32(5)	0.000 05(6)	0.000 10(4)	0.000 15(5)
O1	0.006 7(5)	0.002 3(4)	0.001 5(2)	0.000 6(4)	0.0	0.0
O2	0.004 5(3)	0.003 4(3)	0.002 4(2)	0.000 4(3)	0.000 7(2)	0.000 7(2)

Table 4. Selected bond lengths and angles for $GdAlO_3$ and $GdFeO_3$ perovskite.

Bond (Å) or angle (deg)		$GdAlO_3$	Bond (Å) or angle (deg)		$GdFeO_3$
$[AlO_6]$			$[FeO_6]$		
Al–O1	×2	1.900 74(6)	Fe–O1	×2	2.0010(7)
Al–O2	×2	1.903 62(17)	Fe–O2	×2	2.0101(14)
Al–O2	×2	1.909 68(17)	Fe–O2	×2	2.0299(14)
⟨Al–O⟩		1.905	⟨Fe–O⟩		2.014
Vol (Å)		9.260	Vol (Å)		10.879
O1–Al–O1	×2	180	O1–Fe–O1	×2	180
O1–Al–O2	×2	89.23(12)	O1–Fe–O2	×2	88.67(8)
O1–Al–O2	×2	89.95(11)	O1–Fe–O2	×2	88.31(7)
O1–Al–O2	×2	90.05(11)	O1–Fe–O2	×2	91.69(7)
O1–Al–O2	×2	90.77(12)	O1–Fe–O2	×2	91.33(8)
O2–Al–O2	×2	90.81(2)	O2–Fe–O2	×2	90.29(2)
O2–Al–O2	×2	89.19(2)	O2–Fe–O2	×2	89.71(2)
O2–Al–O2	×2	180	O2–Fe–O2	×2	180
$[GdO_{12}]$			$[GdO_{12}]$		
Gd–O1		2.954(3)	Gd–O1		2.353(2)
Gd–O1		2.416(3)	Gd–O1		2.282(3)
Gd–O1		2.978(3)	Gd–O1		3.179(3)
Gd–O1		2.304(3)	Gd–O1		3.401(2)
Gd–O2	×2	2.515(3)	Gd–O2	×2	2.5452(15)
Gd–O2	×2	2.333(2)	Gd–O2	×2	2.3248(14)
Gd–O2	×2	2.620(2)	Gd–O2	×2	2.6894(14)
Gd–O2	×2	3.151(2)	Gd–O2	×2	3.5268 (16)
Al–O1–Al		156.49(19)	Fe–O1–Fe		146.83(13)
Al–O2–Al		156.35(13)	Fe–O2–Fe		147.37(8)

chip for approximate pressure measurements and a quartz crystal as an internal diffraction pressure standard. A 4:1 mixture of methanol:ethanol was used as the pressure medium. The constant widths of the diffraction peaks at all pressures indicated that this pressure medium remained hydrostatic up to the highest pressures achieved, 7.95 GPa. Diffraction measurements were performed on a Huber four-circle diffractometer. Full details of the instrument and the peak-centring algorithms are provided by Angel *et al* [13]. Unit cell parameters were

Table 5. Unit cell parameters of $GdAlO_3$ measured in the diamond anvil cell from 1 bar to 7.945 GPa. The figures in parentheses represent 1 esd of the last decimal place shown.

Pressure (GPa)	*a*-axis (Å)	*b*-axis (Å)	*c*-axis (Å)	Volume (Å^3)
0.0001	5.2528(3)	5.3018(3)	7.4455(1)	207.350(10)
1.636(2)	5.2407(3)	5.2835(3)	7.4259(2)	205.616(13)
2.568(3)	5.2344(2)	5.2731(2)	7.4151(1)	204.670(9)
3.011(8)	5.2317(2)	5.2682(2)	7.4104(1)	204.241(9)
3.657(5)	5.2278(3)	5.2613(2)	7.4031(1)	203.621(10)
4.412(5)	5.2230(3)	5.2534(2)	7.3945(1)	202.894(10)
4.990(4)	5.2193(3)	5.2474(2)	7.3885(1)	202.351(10)
5.724(6)	5.2151(3)	5.2397(2)	7.3807(1)	201.682(10)
6.541(4)	5.2107(4)	5.2314(3)	7.3715(2)	200.943(15)
6.888(5)	5.2083(3)	5.2283(3)	7.3683(2)	200.641(13)
7.522(8)	5.2052(2)	5.2221(2)	7.3618(1)	200.108(8)
7.945(8)	5.2024(2)	5.2182(2)	7.3574(1)	199.733(8)

Table 6. Unit cell parameters of $GdFeO_3$ perovskite measured in the diamond anvil cell from 1 bar to 7.461 GPa. The figures in parentheses represent 1 esd of the last decimal place shown.

Pressure (GPa)	*a*-axis (Å)	*b*-axis (Å)	*c*-axis (Å)	Volume (Å^3)
0.0001	5.3509(4)	5.612 18(20)	7.670 74(24)	230.354(17)
1.372(2)	5.3384(2)	5.598 09(10)	7.652 13(12)	228.681(9)
2.157(4)	5.3311(2)	5.590 67(12)	7.641 61(15)	227.755(11)
2.495(8)	5.3284(2)	5.587 30(8)	7.637 46(9)	227.378(7)
3.339(3)	5.3209(1)	5.579 37(7)	7.626 37(9)	226.405(6)
4.190(3)	5.3135(1)	5.571 46(8)	7.616 00(9)	225.463(7)
4.840(3)	5.3081(2)	5.565 78(10)	7.608 22(13)	224.773(9)
5.549(6)	5.3023(2)	5.559 33(9)	7.599 81(11)	224.023(8)
6.376(6)	5.2957(2)	5.552 33(9)	7.590 79(11)	223.196(8)
7.017(6)	5.2905(2)	5.546 72(11)	7.583 82(14)	222.545(10)
7.461(6)	5.2871(2)	5.543 14(8)	7.578 88(9)	222.113(7)

determined at each pressure from a least squares fit to the corrected setting angles of 18–20 reflections obtained by the eight-position-centring method [7]. The unconstrained unit cell angles showed no significant deviation from 90°, indicating that the structure remains orthorhombic over the pressure range of our data. The values of symmetry-constrained unit cell parameters obtained by vector least squares fitting [14] for $GdAlO_3$ and GdFeO are reported in tables 5 and 6, respectively. Pressures were determined from the unit cell volumes of the quartz crystal in the diamond anvil cell, using the Birch–Murnaghan third-order equation of state with $K_{T0} = 37.12(9)$ GPa, and $K_0' = 5.99(4)$ [15]. Equation of state parameters were obtained by a weighted least squares fit of the Birch–Murnaghan third-order equation of state to the pressure–volume data [16]. Weights for each datum were calculated by the effective variance method [17] from the esd in the unit cell volume of the perovskites combined with the uncertainty in pressure corresponding to the esd of the unit cell volume of the quartz pressure standard.

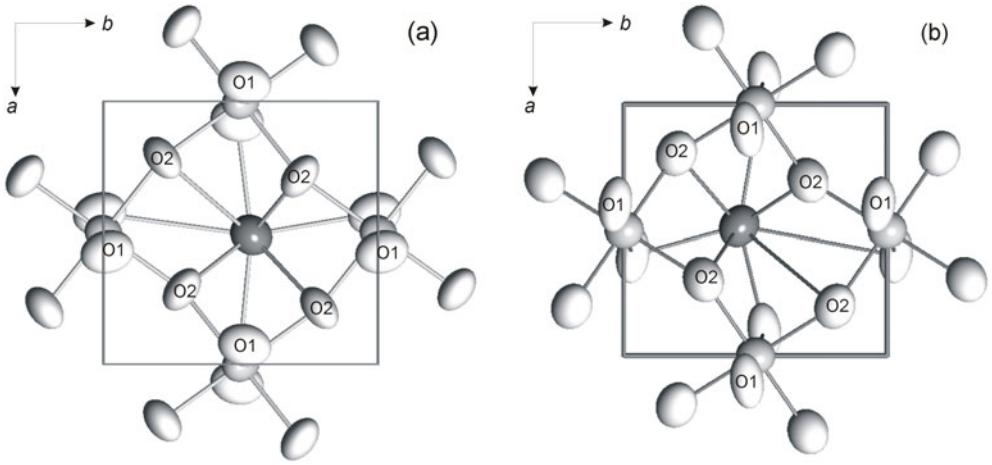

Figure 1. Comparison of the structures of (a) $GdAlO_3$ perovskite and (b) $GdFeO_3$ perovskite viewed onto (001). The oxygen atoms are shown in light grey, the octahedral Al (and Fe) atoms are shown in medium grey and the Gd atoms are shown in dark grey.

3. Comparison of structures

Both $GdFeO_3$ and $GdAlO_3$ crystallize in space group *Pbnm* under ambient conditions. The most prominent distortion from the ideal cubic perovskite involves tilting of the BO_6 octahedra (figure 1). The departure of the interoctahedral angles, B–O1–B and B–O2–B, from 180° in the ideal cubic perovskite structure provides one measure of this distortion. In $GdFeO_3$, the Fe–O1–Fe and Fe–O2–Fe angles are 146.83(13)° and 147.37(8)°, respectively. In $GdAlO_3$, the Al–O1–Al and Al–O2–Al angles are 156.49(19)° and 156.35(13)°, respectively. The value of the O2–O2–O2 angle that shows the degree of tilting in the xy plane is 139.74° in $GdFeO_3$ and 150.65° in $GdAlO_3$, in contrast to 180° for a cubic perovskite. The value of the O2–O2–O2 angle that shows the degree of tilting in the xz plane is 106.26° in $GdFeO_3$ and 102.25° in $GdAlO_3$, in contrast to 90° for a cubic perovskite. The greater distortion of $GdFeO_3$ relative to $GdAlO_3$ is also reflected in the observed tolerance factor, $t_{obs} = \langle A\text{–}O\rangle/\sqrt{2}\langle B\text{–}O\rangle$, where $\langle A\text{–}O\rangle$ and $\langle B\text{–}O\rangle$ are the mean interatomic separations between twelve and six nearest neighbours for the A and B sites, respectively [18]. For a cubic perovskite, $t_{obs} = 1$ but $GdAlO_3$ has $t_{obs} = 0.986$ and $GdFeO_3$ has $t_{obs} = 0.977$.

The distorted orthorhombic structure arises from the discrepancy between the radii of the cations in the AO_{12} and BO_6 sites. The distortion is accompanied by anti-parallel displacements of the Gd atoms in the (001) plane, thereby changing their oxygen environment. Whereas the A cations in the ideal perovskite structure are surrounded by twelve equidistant oxygen anions, the Gd–O distances in $GdFeO_3$ and $GdAlO_3$ are distributed in a range from 2.282(3) to 3.527(12) Å and from 2.304(3) to 3.151(2) Å, respectively (figure 1). The coordination numbers of Gd in the two structures can be approximated from bond valence, s_{ij}, sums and matching them to the oxidation state (V_{ij}) of Gd using the following relationship from Brown and Altermatt [19]:

$$V_{ij} = \sum_j s_{ij} = \sum_j \exp\left[\frac{(r_0' - r_{ij})}{B}\right]. \tag{1}$$

In equation (1), r_0' is the bond valence parameter (2.063 = for Gd^{3+}–O bonds), r_{ij} is the observed bond length and B (=0.37) is an empirically determined parameter [20]. For $GdFeO_3$,

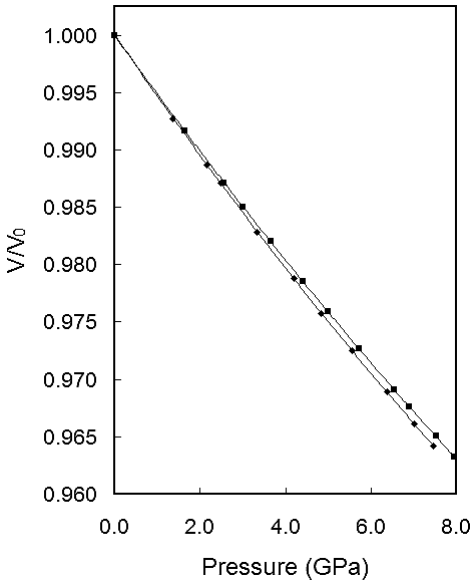

Figure 2. The variation of the unit cell volume of $GdAlO_3$ perovskite (squares) and $GdFeO_3$ perovskite (diamonds) between room pressure and 8 GPa. The size of the symbol shown represents ± 1 esd of the measured V/V_0.

the best match to the oxidation state of Gd is obtained from contributions of the ten nearest neighbour Gd–O separations $\left(\sum s_{ij} = 3.00\right)$. For $GdAlO_3$, the best matches to the oxidation state are obtained from contributions of the nine shortest Gd–O separations $\left(\sum s_{ij} = 3.01\right)$, with a significant portion from the eight nearest neighbours $\left(\sum s_{ij} = 2.92\right)$.

The distortion of the AO_{12} and BO_6 sites can be compared using the bond length distortion parameter, $\Delta = (l/n)\sum\{(r_j - r)/r\}^2 \times 10^3$ where r is an average bond length, r_j is an individual bond length and n is the number of bonds [18]. The FeO_6 octahedra in $GdFeO_3$ are more distorted than the AlO_6 octahedra in $GdAlO_3$, with Δ_B values of 0.036 and 0.004, respectively. Similarly, the GdO_{12} sites are much more distorted in $GdFeO_3$ than $GdAlO_3$, with Δ_A values of 28.33 and 13.16, respectively. Both $GdFeO_3$ and $GdAlO_3$ follow the systematic trends for other *Pbnm* perovskites described by Sasaki *et al* [18].

4. Equations of state

The volumes of $GdAlO_3$ and $GdFeO_3$ decrease smoothly with increasing pressure, with no evidence of any phase transitions throughout the pressure range studied (figure 2). For $GdAlO_3$, the fit of the P–V data collected between room pressure and 7.945(8) GPa yielded room pressure parameters $V_0 = 207.348(9)$ Å^3, $K_{T0} = 191(1)$ GPa and $K_0' = 5.8(3)$ for the third-order Birch–Murnaghan equation of state. For $GdFeO_3$, the fit of the P–V data collected between room pressure and 7.461(6) GPa yielded the following parameters: $V_0 = 230.369(13)$ Å^3, $K_{T0} = 182(1)$ GPa and $K_0' = 6.3(3)$. Figure 3 shows the compression data plotted as the normalized pressure, F, against the Eulerian strain measure, f [16]. F–f plots provide a visual indication of whether higher order terms such as K_0' and K_0'' are significant in the EoS. If all data points lie on a horizontal line of constant F, for example, then $K_0' = 4$, and the data can be fitted with a second-order Birch–Murnaghan EoS. If the data lie on an inclined

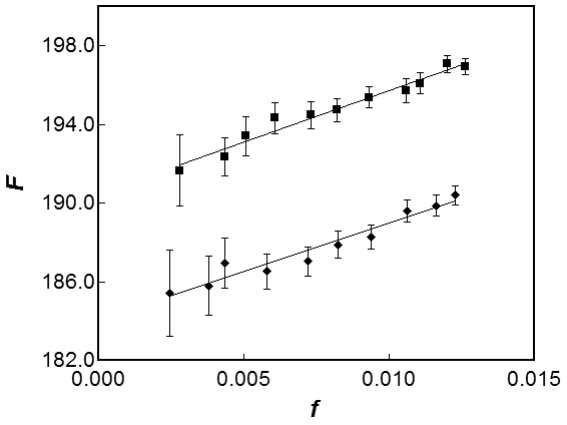

Figure 3. Variation of the normalized pressure, F, against the finite strain, f, for $GdAlO_3$ perovskite (squares) and $GdFeO_3$ perovskite (diamonds). See the text for details.

straight line, as is the case for $GdAlO_3$ and $GdFeO_3$ (figure 3), the data will be adequately described by a third-order truncation of the Birch–Murnaghan EoS with the slope of each line equal to $3K_T(K'-4)/2$. Figure 3 therefore provides visual confirmation that K'_0 is significantly greater than 4 for $GdAlO_3$ and $GdFeO_3$, similar to the case for other orthorhombic perovskites with $K'_0 = 6$ [21–25]. Fitting the data for any of these materials with a second-order EoS (i.e. $K'_0 = 4$) leads to significantly worse fits to the data and significant overestimates of the bulk moduli.

The elastic moduli of the individual unit cell axes of $GdAlO_3$ and $GdFeO_3$ perovskite were also obtained from the measured data by fitting a third-order Birch–Murnaghan equation of state to the cubes of each of the cell parameters in turn [16]. The resulting axial moduli (K_{d0}) and their pressure derivatives (K'_{d0}) are: $K_{a0} = 234(5)$ GPa, $K_{b0} = 151(2)$ GPa and $K_{c0} = 205(1)$ GPa, with $K'_{a0} = 12(1)$, $K'_{b0} = 3.8(4)$ and $K'_{c0} = 4.7(2)$ for $GdAlO_3$, compared with $K_{a0} = 188(3)$ GPa, $K_{b0} = 181(1)$ GPa and $K_{c0} = 177(2)$ GPa, with $K'_{a0} = 5.2(7)$, $K'_{b0} = 5.7(4)$ and $K'_{c0} = 8.2(5)$ for $GdFeO_3$. The a-axis is the least compressible axis in both structures, followed by c then b for $GdAlO_3$ and by b and c for $GdFeO_3$. The maximum anisotropy in the compressional moduli is about 35% for $GdAlO_3$ (for a-axis to b-axis) and only 6% for $GdFeO_3$ (for a-axis to c-axis). Whereas $GdFeO_3$ displays anisotropic compression that is similar to those of other orthorhombic perovskites, $GdAlO_3$ displays one of the largest anisotropic compressibilities for any orthorhombic perovskite yet measured. The pressure derivatives of the axial moduli also show the greatest variation for $GdAlO_3$, ranging from 4 (b-axis) to 12 (a-axis), compared with the $GdFeO_3$ case, where they range from 5 (a-axis) to 8 (c-axis).

5. Discussion

Zhao *et al* [25] used the bond valence concept to develop a model that predicts the relative compressibilities of the cation sites in oxide perovskites. They introduced a parameter M_i for the octahedral and dodecahedral sites defined in terms of the coordination number N_i, average bond length at room pressure R_i and bond valence parameters R_0 and B [19, 20]:

$$M_i = \frac{R_i N_i}{B} \exp\left(\frac{R_0 - R_i}{B}\right). \tag{2}$$

M_i represents the variation of the bond valence sum at the central cation in a polyhedral site due to the change of the average bond distance. Experimental data suggest that the pressure-induced changes in the bond valence sums at the two cation sites within any given perovskite are

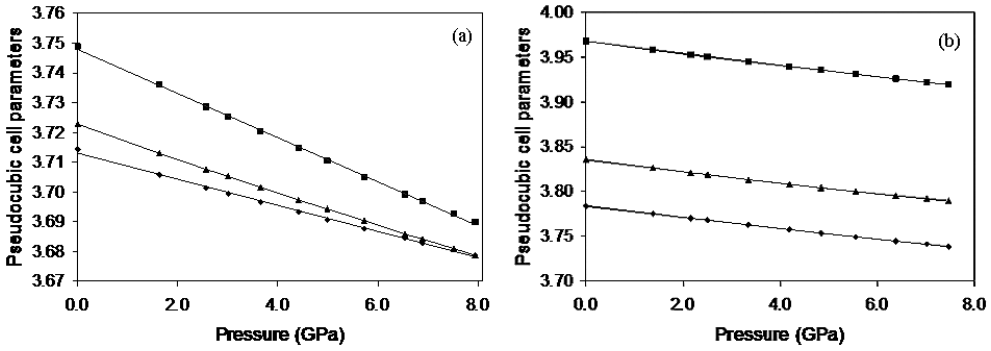

Figure 4. The variation of the pseudocubic unit cell parameters, a_c, b_c, and c_c (Å) of (a) $GdAlO_3$ perovskite and (b) $GdFeO_3$ perovskite between room pressure and 8 GPa. The axes are represented by the following symbols: a_c: diamonds; b_c: squares; and c_c: triangles.

equal. With this condition, Zhao *et al* [25] showed that the ratio of cation site compressibilities is given by

$$\beta_B/\beta_A = M_A/M_B. \tag{3}$$

This model, based only upon room pressure bond lengths and bond valence parameters, correctly predicts the structural behaviour and some physical properties of the oxide perovskites that have been measured at high pressure.

For $GdAlO_3$, $R_0 = 1.651$, $B = 0.37$, $R_i = 1.905$ and $M_B = 15.55$ for the AlO_6 site and $R_0 = 2.065$, $B = 0.37$, $R_i = 2.658$ and $M_A = 20.67$ for the GdO_{12} site. For $GdFeO_3$, $R_0 = 1.759$, $B = 0.37$, $R_i = 2.014$ and $M_B = 16.39$ for the FeO_6 site and $R_0 = 2.065$, $B = 0.37$, $R_i = 2.782$ and $M_A = 18.89$ for GdO_{12}. The ratios of M_A/M_B are therefore 1.33 and 1.15 for $GdAlO_3$ and $GdFeO_3$, respectively. The fact that M_A/M_B takes values greater than 1 suggests that the octahedral BO_6 site should be more compressible than the AO_{12} site and therefore the structure will become less distorted with increasing pressure. There is also a close relation between the value of M_A/M_B and the degree of pressure-induced distortion and tilting in the $GdFeO_3$-type perovskites [25]. Perovskites with greater M_A/M_B values show a greater degree of distortion with pressure. Thus $GdAlO_3$, which has a greater M_A/M_B (1.33) than $GdFeO_3$ (1.15), should display a greater change in the degree of distortion, becoming less distorted than $GdFeO_3$ over a similar pressure range. This is reflected in the pseudocubic unit cell parameters, $a/\sqrt{2}$, $b/\sqrt{2}$, $c/2$, that show a greater variation with pressure in $GdAlO_3$ than $GdFeO_3$ (figure 4). The metrical deviation of the orthorhombic perovskite from tetragonal symmetry is proportional to $(b-a)/a_0$ where a_0 is the value in the high symmetry (in this case, tetragonal) phase (e.g. [26]). It is clear from figure 4 that the tetragonal–orthorhombic strain is decreasing with increasing pressure. If the linear trends of $a/\sqrt{2}$ and $b/\sqrt{2}$ are extrapolated to higher pressure, they converge at 11.6 GPa where the strain would go to zero. Further structural studies are needed to verify whether aluminate perovskites display a decrease in distortion with increasing pressure and whether a phase transition occurs in $GdAlO_3$ perovskite at higher pressure.

It is interesting to compare the K_T values of the 3–3 perovskites with those of 2–4 perovskites such as the $CaBO_3$ series (B = Zr, Sn, Ti, Ge). Zhao *et al* [25] observed that there is a correlation between M_A/M_B ratios (which are all <1) and the bulk moduli of Ca oxide perovskites. On the basis of limited data, it appears that a trend also exists for $AAlO_3$ perovskites (A = Gd, Y, Sc), which all have $M_A/M_B > 1$ (figure 5). The linear trend, K_T (GPa) $= 319.19 - 96.367(M_A/M_B)$, may be useful in providing an estimate of the bulk modulus of other *Pbnm* aluminate perovskites. For example, we would predict that $SmAlO_3$

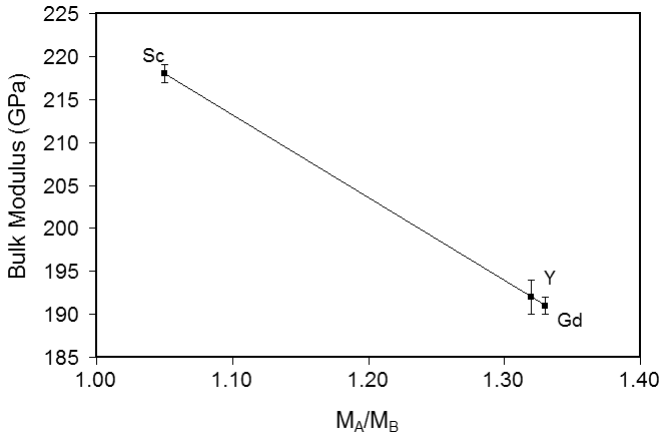

Figure 5. A plot of the isothermal bulk moduli, K_T, of $ScAlO_3$ [27], $YAlO_3$ [24] and $GdAlO_3$ perovskite (this study) as a function of their M_A/M_B ratios.

($M_A/M_B = 1.31$) would have a bulk modulus of 193 GPa. Further work is needed to verify whether this trend holds for other orthorhombic aluminate perovskites, as well as aluminate perovskites with different symmetries.

Acknowledgment

NLR and JZ gratefully acknowledge support from NSF grant EAR-0408460.

References

[1] Glazer A M 1972 *Acta Crystallogr.* B **28** 3384
[2] Woodward P M 1997 *Acta Crystallogr.* B **52** 32
[3] Woodward P M 1997 *Acta Crystallogr.* B **53** 44
[4] Navrotsky A and Weidner D 1989 *Geophysical Monograph* vol 45 (Washington, DC: American Geophysical Union)
[5] Geller S 1956 *J. Chem. Phys.* **24** 1236
[6] Marezio M, Remeika J P and Dernier P D 1970 *Acta Crystallogr.* B **26** 2008
[7] King H E and Finger L W 1979 *J. Appl. Crystallogr.* **12** 374
[8] Angel R J 2003 *J. Appl. Crystallogr.* **36** 295
[9] Pavese A and Artioli G 1996 *Acta Crystallogr.* A **52** 890
[10] Angel R J 2004 *J. Appl. Crystallogr.* **37** 486
[11] Finger L W and Prince T E 1975 *NBS Technical Note, 854,* US National Bureau of Standards, Washington, DC
[12] Allan D R, Miletich R and Angel R J 1996 *Rev. Sci. Instrum.* **67** 840
[13] Angel R J, Downs R T and Finger L W 2000 *Rev. Mineral. Geochem.* **41** 559
[14] Ralph R L and Finger L W 1982 *J. Appl. Crystallogr.* **15** 537
[15] Angel R J, Allan D T, Militech R and Finger L W 1997 *J. Appl. Crystallogr.* **30** 461
[16] Angel R J 2000 *Rev. Mineral. Geochem.* **41** 35
[17] Orear J 1982 *Am. J. Phys.* **50** 912
[18] Sasaki S, Prewitt C T and Liebermann R C 1983 *Am. Mineral.* **68** 1189
[19] Brown I D and Altermatt D 1985 *Acta Crystallogr.* B **41** 244
[20] Brese N E and O'Keeffe M 1991 *Acta Crystallogr.* B **47** 192
[21] Ross N L and Angel R J 1999 *Am. Mineral.* **84** 277
[22] Kung J, Angel R J and Ross N L 2000 *Phys. Chem. Minerals* **28** 35
[23] Ross N L and Chaplin T D 2003 *J. Solid State Chem.* **172** 123
[24] Ross N L, Zhao J and Angel R J 2004 *J. Solid State Chem.* **177** 1276
[25] Zhao J, Ross N L and Angel R J 2004 *Acta Crystallogr.* B **60** 263
[26] Redfern S A T 1996 *J. Phys.: Condens. Matter* **8** 8267
[27] Ross N L 1998 *Phys. Chem. Minerals* **25** 597